International Journal of Nanomedicine

Dovepress
Taylor & Francis Group

Open Access Full Text Article

ORIGINAL RESEARCH

A Baicalin Liposome-Based Temperature-Sensitive Hydrogel for Treating Ultraviolet-Induced Skin Damage

Xing Liu[1], Wenlin Shu[1], Qingrui Zhong[1], Anqi Zeng[2], Yong Zeng[1], Huan Gu[3], Ping Chen[2], Xiaofang Li[1]

[1]State Key Laboratory of Southwestern Chinese Medicine Resources, School of Pharmacy, Chengdu University of Traditional Chinese Medicine, Chengdu, 611137, People's Republic of China; [2]Translational Chinese Medicine Key Laboratory of Sichuan Province, Sichuan Academy of Chinese Medicine Sciences, Chengdu, 610041, People's Republic of China; [3]College of Pharmacy and Food, Southwest Minzu University, Chengdu, 610225, People's Republic of China

Correspondence: Ping Chen; Xiaofang Li, Email 284529046@qq.com; lixiaofang@cdutcm.edu.cn

Purpose: Prolonged exposure of the skin to ultraviolet (UV) rays from sunlight causes oxidative damage to skin cells, and prolonged exposure to UV can lead to severe sunburn and skin aging, which may increase the risk of skin cancer. Numerous natural products have been used to treat UV-induced skin damage. Baicalin (BA) has excellent antioxidant properties; however, its poor solubility hinders its direct application. Therefore, suitable formulations for dermal administration must be developed.

Methods: We designed a temperature-sensitive gel drug delivery system based on baicalin liposome (BA-LP), which was first constructed using lecithin loaded with insoluble BA. Subsequently, an injectable hydrogel (BA-LG) with temperature-sensitive properties was constructed using BA-LP and chitosan (CS) with β-glycerophosphate tetrahydrate (β-GP) as a crosslinking agent.

Results: BA-LP had homogeneous particle size, high EE, and good stability. BA-LG could be gelled within 2 min at 37 °C and had good spreading, adhesion, and injectability properties. The in vitro release results showed that BA-LG had a significantly slower release effect, with a cumulative release of 60% at 24 h. The effects of BA-LG on skin keratinocyte HaCaT cells were evaluated using the CCK8 method and transwell co-culture, and the results showed good cell activity and a high survival rate, indicating that the hydrogel has good biosafety. In the UVB-induced skin injury mouse model, BA-LG showed significant effects by increasing superoxide dismutase (SOD) activity, decreasing malondialdehyde (MDA) damage, and inhibiting the expression of inflammatory factors IL-6, PGE2, and TNF-α, and demonstrated a superior therapeutic effect. The analysis of histopathological sections of the skin stained with H&E and Masson revealed results consistent with those observed on the mice.

Conclusion: In summary, our results suggest that BA-LG, a temperature-sensitive gel based on baicalin liposomes, has good therapeutic efficacy and potential applications in the treatment of UVB-induced skin damage.

Keywords: baicalin, temperature sensitivity, liposome, hydrogel, UV damage, antioxidant

Introduction

The skin is the outermost organ of the human body and plays a vital role in protecting the body from potential harm from the external environment.[1,2] Ultraviolet (UV) rays from sunlight are mainly categorized into UVA (315–400 nm), UVB (280–315 nm), and UVC (200–280 nm), of which UVC is absorbed by the ozone layer of the atmosphere; thus, the skin is mainly exposed to UVA and UVB. UV irradiation causes oxidative damage to skin cells and also causes DNA damage.[3–5] Approximately 70–80% of UVA is absorbed by the epidermis, while the rest penetrates the dermis and causes photoaging of the skin.[6] Short-term exposure to UVA is not a significant risk, causing only melanin deposition, skin aging and hyperpigmentation. However, prolonged exposure to UVA induces the production of ROS, which can damage DNA and proteins and increase the risk of skin cancer.[7] In the case of UVB, short-term exposure is beneficial as it helps in vitamin D synthesis. However, prolonged exposure to UVB causes accumulation of ROS in the epidermis and

Received: 9 January 2025
Accepted: 9 June 2025
Published: 19 June 2025

Graphical Abstract

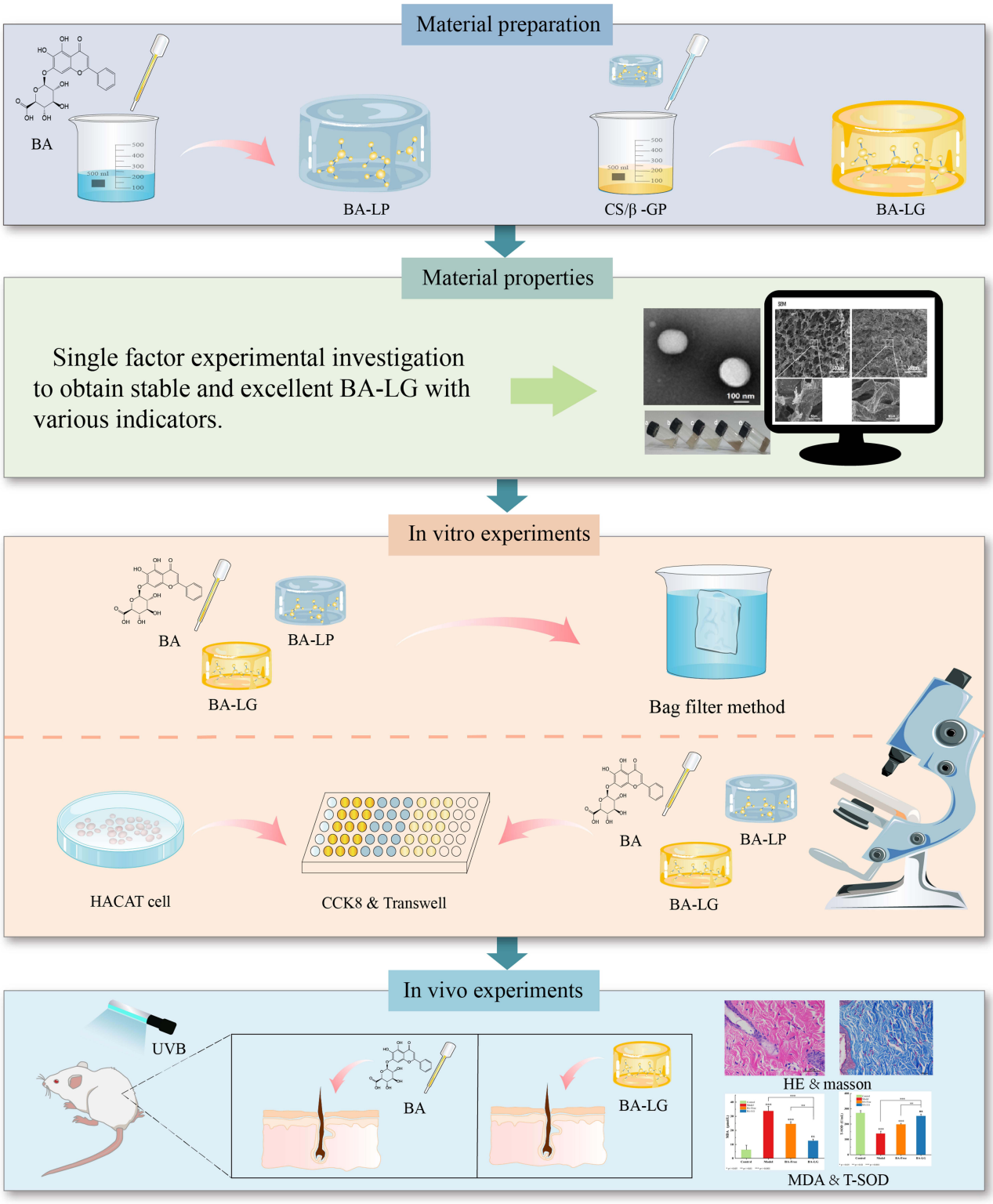

reduction of antioxidant enzyme activity, leading to epidermal damage.[8] UVB also induces DNA damage and increases the risk of skin cancer.[9] Studies have shown that the increasing incidence of skin diseases caused by exposure to UV rays has become an important global health issue.[10,11]

Numerous natural products have been used to treat UV-induced skin damage.[12] Baicalin (BA), a flavonoid isolated from the dried roots of *Scutellaria baicalensis*, a dicotyledonous plant belonging to the Lamiaceae family, has antibacterial, anti-inflammatory, and antioxidant effects.[13,14] Studies have shown that BA can reduce reactive oxygen species (ROS) production and skin cell inflammation, and enhance cell viability.[15,16] In the treatment of light-source dermatoses, BA exhibits photoprotective activity against UVB radiation, inhibits UVB-induced photodamage and apoptosis in the human immortal keratinocyte line (HaCaT), and alleviates epidermal hyperplasia and collagen fiber breakage to a certain extent.[17,18] This protective effect is important for the prevention and treatment of UVB-induced skin damage and related diseases. In addition, BA can exert therapeutic effects via inhibition of the Wnt signaling pathway and inhibition of the Th17/IL-17 axis through activation of PPARγ, exhibiting anti-inflammatory activity that can be leveraged for the treatment of dermatological diseases such as psoriasis.[19] These studies suggest that BA has promising potential in the treatment of skin diseases, especially photodermatoses. Although BA has excellent antioxidant properties, its widespread use in therapeutic applications remains challenging because of its poor solubility. Studies have been conducted to design new delivery modes for BA and to develop strategies to improve its solubility, including the formation of liposomes, phospholipid complexes, solid nanocrystals, and micelles.[20–23]

Dermal modes of drug delivery usually include topical and transdermal delivery.[24] Topical administration involves uniform application of the drug to the surface of the skin, whereas transdermal administration increases the skin barrier penetration of the drug and improves the bioavailability of the drug.[25] The use of physical penetration or chemical penetration enhancers is the conventional method to penetrate and weaken the stratum corneum, but they are more damaging and irritating to the skin.[26,27] In contrast, newer delivery systems such as particles and phospholipids can be more gentle and effective for transdermal drug delivery, and are one of the promising modes of dermal drug delivery.[28–30] A liposome is a delivery system consisting of a phospholipid bilayer, similar in structure and composition to a cell membrane. It is therefore amphiphilic and can be used as a delivery vehicle for both hydrophilic and lipophilic drugs.[31] In addition, its phospholipid layer can readily bind to skin lipids and maintain the required hydration conditions, thereby improving drug penetration and localization in the skin layer.[32] However, liposomes do not retain well as a liquid on the skin surface, and therefore their traditional delivery form needs to be modified to increase retention on the skin surface and thereby increase efficacy.

Nanohydrogels have exhibited abilities to accelerate the healing of damaged skin, attenuate skin photoaging, improve drug delivery efficiency, and target skin cancers; therefore, nanohydrogels have recently been widely used in the treatment of UV-damaged skin.[33–36] Recently, nanohydrogels with temperature-sensitive properties have also been investigated.[37] As a smart nanomaterial, a temperature-sensitive gel is unique in its ability to change its physical state in response to changes in ambient temperature. At lower or storage temperatures, temperature-sensitive gels remain in a sol-gel state with good fluidity, similar to that of a liquid.[38] However, when the temperature increases to the phase-change temperature (typically the human body temperature), the gel changes to a solid/semi-solid gel with some viscoelasticity and rapid self-recovery. This temperature-responsive transition not only enables the temperature-sensitive gel to undergo a rapid sol-to-gel transition on the skin surface but also significantly enhances adhesion at the site of administration and thereby prolonging the retention time of the drug at the site of action.[39,40] These properties of temperature-sensitive gels make them important in drug delivery systems, especially for local drug delivery, where they can release drugs directly at the site of the lesion, increase local drug concentration, and reduce the adverse effects of systemic drug delivery.[41,42] In addition to this, it provides multiple options for drug delivery systems with different routes of administration, indicating a wide range of application prospects in clinical medicine, bioengineering, tissue engineering, and other fields. In summary, optimal formulations for skin drug delivery can be developed by improving BA solubility.[43–45] In this study, we designed a temperature-sensitive gel system based on baicalin liposomes (BA-LP) to enable efficient delivery of drugs at the target site for the treatment of UV-induced skin damage, thereby improving the therapeutic effect.

Materials and Methods

Materials

Baicalin (BA), cholesterol, and β-glycerophosphate tetrahydrate (β-GP) were purchased from Yuanye Biotechnology Co., Ltd (Shanghai, China). Chitosan (CS, deacetylation degree ≥95%, viscosity 100–200 mpa.s) was purchased from Aladdin Biochemical Technology Co. Ltd. (Shanghai, China). Soybean phospholipids were purchased from AVT Pharmaceutical Tech Co., Ltd. (Shanghai, China). DMEM medium, fetal bovine serum (FBS), and penicillin–streptomycin were purchased from Gibco (CA, USA). CCK-8 was supplied by Biosharp (Shanghai, China). Superoxide dismutase (SOD), glutathione (GSH), hydrogen peroxide (H_2O_2), and malondialdehyde (MDA) kits were purchased from Jiancheng Bioengineering Institute (Nanjing, China). BCA protein assay kit was obtained from Labgic Technology Co., Ltd. (Beijing, China).

Preparation of BA-LP

BA-LP was prepared using a thin-film hydration method.[46,47] Briefly, soy lecithin, cholesterol, and BA were weighed and added to a round-bottom flask, and organic solvents were added to dissolve them under sonication in a water bath. The organic solvents were removed by evaporation under reduced pressure at 37 °C using a rotary evaporator (Yarong Biochemical Instrument Factory, China), resulting in the formation of a homogeneous, transparent lipid film. Then, PBS (pH=7.2) was added to the film for hydration at the indicated temperature. After hydration was completed, BA-LP was obtained by sonicating for 10 min using an ultrasonic crusher (Safer Co., Ltd., China) in an ice bath for homogenization.

Factors Affecting BA-LP Properties

During liposome preparation, it is important to determine the effect of each independent factor on the BA-LP preparation. Therefore, several factors were examined, including BA-to-soy lecithin mass ratio (BA/LEC), soy lecithin-to-cholesterol (LEC/CHO) mass ratio, type of organic solvent, hydration volume, hydration temperature, and hydration time. To determine the effect of each individual factor on the encapsulation efficiency, particle size, and PDI of BA-LP, we conducted a series of trials wherein each individual factor was varied while the other factors were kept constant.

Characterization of BA-LP

Particle Size, PDI

Particle size, PDI of BA-LP were determined at 25 °C using a particle size and potential analyzer (NICOMP 380 ZLS, PSS, US).

Encapsulation Efficiency and Drug Loading

The encapsulation efficiency (EE%) of BA-LP were determined using latex-breaking centrifugation, disruption of liposomes by the addition of methanol, and ultrasonic extraction of BA, followed by high-performance liquid chromatography (HPLC) to determine the amount of BA in BA-LP. Briefly, 1 mL of BA-LP was weighed precisely and centrifuged at 4000 r/min for 30 min; 1 mL of the supernatant was aspirated, diluted with methanol, and then volumetrically discharged into a 10 mL volumetric flask. After filtered through 0.22 μm microporous membrane, the content of free BA (M_F) was determined by HPLC. In addition, 1 mL of BA-LP was weighed, dissolved in methanol by ultrasonication for 30 min as described above, and then filtered through a 0.22 μm microporous filter membrane, and the total amount of BA (M) in the suspension was determined by HPLC. Encapsulation efficiency and drug loading were calculated as follows:

$$EE\% = (M - M_F) / M \times 100\%$$

where M is the total BA content in BA-LP, M_F is the free BA content in BA-LP.

Stability of BA-LP

The prepared BA-LP were stored at 4 °C for 14 days. The particle size, PDI, and encapsulation efficiency of BA-LP were measured on days 1–7 and day 14 to examine the stability.

Transmission Electron Microscope Analysis

The morphology of BA-LP was examined using a transmission electron microscope (TEM) (JEM-2100F, JEOL, Japan) operated at an accelerating voltage of 200 kV. Prior to obtaining the imaging, the samples were negatively stained with 2% (v/v) phosphotungstic acid for 5 min, added dropwise to a copper grid, and dried at room temperature.

Preparation of Temperature-Sensitive Hydrogels

The gel solution was prepared following the chitosan/β-glycerophosphate tetrahydrate (CS/β-GP) cold method.[48,49] CS was weighed precisely and dissolved in 0.1 mol/L aqueous acetic acid solution for injection to obtain chitosan acetic acid solution. The prepared BA-LP was added dropwise to the solution under stirring on an ice bath, and stirring was continued until the mixture was homogeneous, after which it was set aside. In parallel, β-GP was precisely weighed and dissolved in 0.1 mol/L sodium bicarbonate solution, and ultrasonicated until complete dissolution. This β-GP solution was added dropwise to the chitosan solution containing BA-LP on an ice and stirred thoroughly to obtain a free-flowing clear solution, and the pH of the solution was adjusted to approximately 7.1 using 0.1 mol/L sodium bicarbonate. The solution thus obtained was the temperature-sensitive baicalin liposome hydrogel (BA-LG) pre-solution. The BA-LG pre-solution was maintained at 37 °C to allow gelation to form BA-LG.

Analysis of Factors Affecting Gelation Time and Temperature

During the preparation of temperature-sensitive gels, it is important to determine the effect of each independent factor on the preparation of BA-LG. Therefore, the factors—CS concentration, β-GP solution concentration, and chitosan solution to β-GP solution volume ratio—were examined. A one-way experiment was conducted to determine the effect of each factor on the gelling temperature and gelling time of BA-LG. The prepared BA-LG was placed in a thermostatic water bath at 35 °C, and the temperature was increased at the rate of 0.5 °C per 10 min. The vials were inverted every 10s to observe the fluidity of the pregel solution until the gel did not flow when the vials were inverted, and the gelling temperature and gelling time were recorded.

Characterization of BA-LG

The gelling temperature and time and pH of the prepared BA-LG samples were determined. The color, appearance, homogeneity, pH, diffusivity, injectability, adhesion, and spreadability of the prepared gels were evaluated.

The pH of BA-LG was measuring by a pH meter. The microscopic morphology of the BA-LG surface was observed using a scanning electron microscope.

To examine the gel spreadability, a 1 g sample of BA-LG gel was placed in a circle of 1 cm diameter on a glass plate, and the spreadability was determined by placing different weights of the glass plate on the gel. This was done by placing 50 g, 100 g, 150 g and 200 g weights at 1 min intervals and measuring the diameter of the altered horizontal and vertical axes of the gel after 1 min, and then calculating and analyzing the change in gel area with respect to the weight.[50]

In vitro Release

The dialysis bag method was used to determine the in vitro cumulative release rate and to investigate the sustained-release effect of BA-LG.[51–53] The dialysis bag method was used to determine the in vitro cumulative release rate and to investigate the controlled-release effect of BA-LG. First, 3 mL each of free baicalin (BA-Free), BA-LP, and BA-LG were taken, of which BA-LG had undergone complete gelation at 37 °C in a water bath, placed in a dialysis bag, and sealed. The dialysis bag was placed in 50 mL of PBS (pH 7.2). The in vitro release experiment was performed at 37 °C at a stirring rate of 50 rpm. The BA content was determined by taking 1 mL of dialysate at 0.5, 1, 2, 4, 6, 12, and 24 h, and replacing 1 mL of fresh PBS solution at the same temperature to maintain the total volume of 50 mL. The BA concentration at each sampling point was determined using HPLC to calculate the cumulative release. Each experiment was performed in triplicate.

In vitro Transdermal Penetration

After anesthetizing SD rats, the abdominal hair was removed using a mild depilatory cream. The rats were executed after 24 h. The abdominal skin and adherent subcutaneous tissues on the visceral side of the skin were surgically excised and the remaining adherent subcutaneous tissues and fat were removed by wiping with physiological saline. After the skin was finally washed again with PBS, it was carefully examined with a magnifying glass to ensure the absence of any surface irregularities. The treated clean rat skin was hydrated in PBS for 24 h and placed in a Franz diffusion cell so that the stratum corneum side was facing the donor compartment and the dermis side was facing the recipient compartment, with an effective diffusion surface area of 1.76 cm^2. The recipient compartment of the diffusion cell was filled with PBS containing 1% Tween 80, the aqueous bath temperature was maintained at 36.5 ± 0.5°C, and a magnetic stirrer was used for continuous 300 rpm/min Stirring.

BA-Free, BA-LP, and BA-LG were uniformly applied to the skin of the donor chamber and sealed with plastic wrap to provide containment. 200 μL of recipient chamber samples were collected at the 0.5, 1, 2, 4, 6, 12, and 24 h time points and supplemented with equal amounts of fresh PBS to maintain recipient chamber conditions.

The BA concentration at each sampling point was determined using HPLC to calculate the cumulative release. Each experiment was performed in triplicate.

Cytotoxicity

HaCaT cells were obtained from the Shanghai Cell Bank of the Chinese Academy of Sciences. Cells were cultured in DMEM supplemented with 10% fetal bovine serum and 1% penicillin–streptomycin at 37 °C under 5% CO_2.

The cytotoxicity of the gel was tested using HaCaT cells. Cells were seeded in 96-well plates at a density of 6000 cells/well. After 24 h, different concentrations of BA-LP and BA-LG were added, followed by incubation for 24 h. Then, 10% CCK8 was added, and absorbance values were read at 450 nm after 1 h.

Using Transwell chambers, cells were inoculated at a density of 20,000 cells/well at the bottom of a 24-well Transwell plate. After 24 h, blank gels (Blank-Gel) and BA-LG gels were added to the inserts, and cells were incubated for a further 24 h. Cell morphology changes were observed using a microscope. After image acquisition, 10% CCK8 was added to each well and the absorbance value was read at 450 nm after 1 h of incubation.

Animal Experiments

Male ICR mice (18–22 g) were purchased from ENSIWEIER Biotechnology (Chengdu, China). All animals were housed under constant conditions (temperature, 25 ± 1 °C; humidity, 50 ± 5%; 12-h light/dark cycle) with free access to standard laboratory diet and water.

After 7 days of acclimatization, the mice were randomly divided into the following four groups: blank (Control), model (Model), free (BA-Free), and gel (BA-LG). The Control group received no treatment or UVB irradiation, the Model group received only UVB irradiation, the BA-Free group received UVB irradiation and BA-Free treatment, and the BA-LG group received UVB irradiation and BA-LG treatment. The experiments were conducted for 7 days for all groups. For administration, the drug concentration in each group was based on the amount of BA in the BA-LG group (380 μg/mL). The administered dose was calculated as 0.1 mL/cm^2. Before the experiment, hair was removed using a soft, gentle, and non-irritating depilatory cream on an area of approximately 2×3 cm^2 on the backs of the mice to expose skin. The mice were observed for the next 48 h to exclude mice exhibiting abnormal hair growth or adverse reactions to the depilatory cream. A UV lamp with an emission wavelength of 313 nm was used as the UVB light source. The UV lamp was equipped with a UV illuminometer to measure the intensity of the incident UV light. The distance between the UVB lamp and the skin on the back of the mice was 40 cm. The mice were irradiated for 30 min using UVB at an intensity of 500 μW/cm^2 to obtain a daily UV irradiation dose of 900 mJ/cm^2.[54]

After 7 days of treatment according to the above experimental scheme, the mice were sacrificed. The skin from the exposed area of the mice was removed, cleaned with normal saline, and fixed in 4% paraformaldehyde for 24 h.

All animal studies were conducted in accordance with the protocols approved by the Animal Welfare Committee of Sichuan Academy of Chinese Medicine Sciences. The laboratory animal welfare guideline followed in this study is Laboratory animals - General code of animal welfare (GB/T 42011–2022).

Histological Analysis

The previously collected mouse skin tissues dehydrated and embedded in paraffin according to standard procedures to make sections. Sections were stained with hematoxylin and eosin (H&E) and Masson's trichrome respectively to analyze the histological characteristics of the skin.

Antioxidant Properties of Skin Lipids

Antioxidant activity was determined by measuring the levels of SOD and MDA in skin tissue using detection kits (Jiancheng BioTech, Nanjing, China) following manufacturer's instructions.

Anti-Inflammatory Properties of BA-LG

Appropriate amount of mouse skin tissue was weighed and ground by adding 9-fold saline, then the grinding solution was centrifuged at 4000 rpm for 10 min at 4°C, and the supernatant was taken to prepare a 10% tissue homogenate. The levels of pro-inflammatory cytokines IL-6, PGE2 and TNF-α in mouse skin tissues were measured using an Elisa kit (Elabscience) according to the manufacturer's instructions.

Statistical Analysis

All experimental data were expressed as the mean ± SD of at least three experiments. Comparisons of other effects were performed using one-way ANOVA. The significance level was set at $p< 0.05$.

Results

Preparation of BA-LP

The single-factor investigation of BA-LP showed that the encapsulation efficiency of BA-LP increased and particle size decreased with an increase in the soybean lecithin-to-BA mass ratio (Figure 1A). This is because the liposomes provide sufficient phospholipid bilayers to encapsulate drugs at high phospholipid concentrations.[55] When investigating the effect of the phospholipid-to-cholesterol mass ratio on BA-LP, we found that the highest EE and smallest particle size were achieved at a ratio of 5:1 (Figure 1B). Because the fluidity, rigidity, permeability, and transition temperature of the

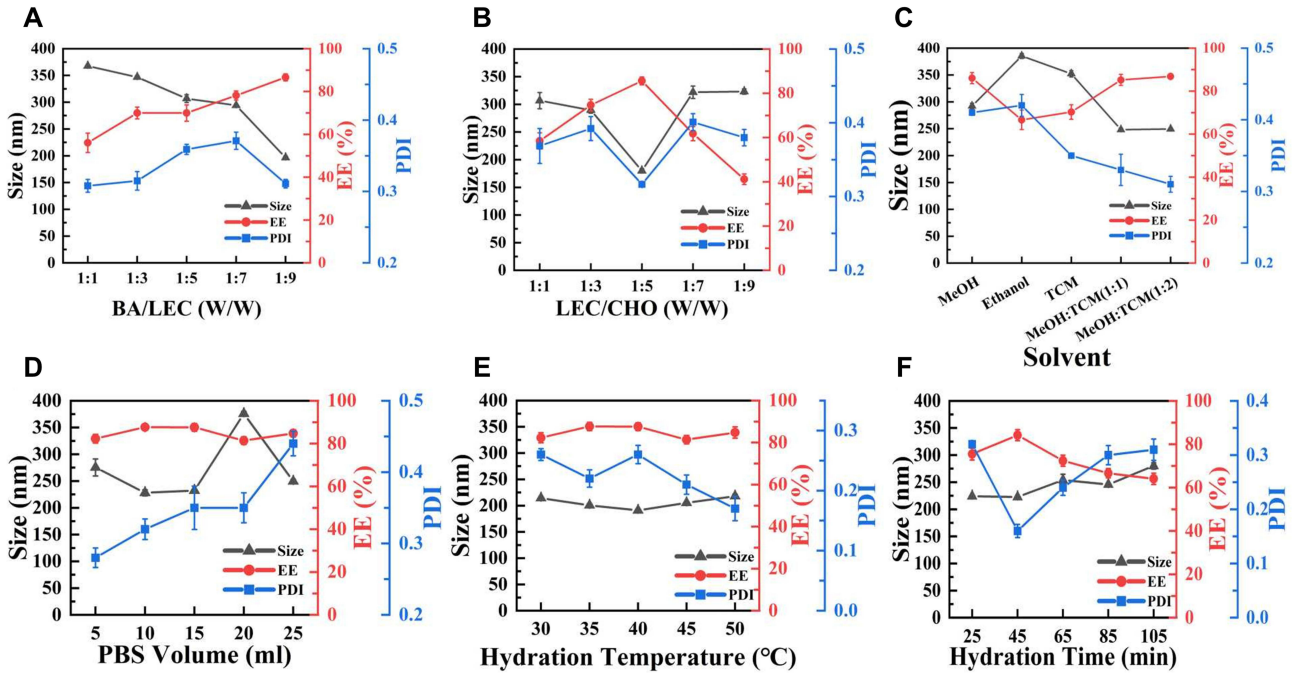

Figure 1 Results of one-way examination of BA/LEC (**A**), LEC/CHO (**B**), type of organic solvent (**C**), hydration volume (**D**), hydration temperature (**E**), and hydration time (**F**).

https://doi.org/10.2147/IJN.S516572

phospholipid bilayer improves with an increase in cholesterol content, its hydrophobic chain is not easily broken, thus maintaining a complete bilayer structure with good fluidity, thereby improving the EE and particle size of liposomes.[56,57] However, when the proportion of cholesterol is too high, it competes with BA for the hydrophobic space of the bilayer and simultaneously destroys the regular and continuous structure of the phospholipid layer, resulting in drug leakage and a lower EE.[58–60] The solubility of materials in organic solvents is also an important factor that affects liposome formation.[61] Baicalin is insoluble in alcohol and only slightly soluble in chloroform, whereas lipid substances, such as phospholipids, are easily soluble in both methanol and chloroform. Therefore, when a mixture of methanol and chloroform (1:2) was used, these lipid-soluble substances showed the best solubility and formed a better phospholipid bilayer with BA (Figure 1C).

Similarly, the hydration conditions have a significant influence on liposome preparation. If the hydration volume is too large, the lipid concentration is low, and more water phase is encapsulated, making the size of the liposomes larger or even disrupting the formation of liposomes. Therefore, when the hydration volume is reduced, the liposomes have a more compact structure, are more stable, and have a smaller particle size. However, it should be noted that the lipid concentration is too high when the hydration volume is too small; in such a situation, the lipid viscosity is high and cannot be adequately dispersed in the aqueous phase and will consequently affect the liposome-forming process (Figure 1D).

The results regarding the effect of hydration temperature showed that the particle size of BA-LP first decreased and then increased with increasing temperature (Figure 1E). This is because an appropriate increase in temperature reduces the rigidity of phospholipids and increases their fluidity to form vesicular structures with smaller particle sizes. However, when the temperature is continuously increased, the physical structures of the phospholipids and cholesterol is disrupted, resulting in the formation of oversized liposomes. Examination of the hydration time showed that the BA-LP particle size decreased with increasing hydration time, whereas the EE decreased (Figure 1F). This is because sufficient hydration can better segment the phospholipid bilayer to form smaller vesicle structures; however, prolonged hydration also increases BA leakage, thus affecting the EE.

Based on the validation examination of the single-factor results, we determined the optimal process for the preparation of BA-LP and characterized the prepared BA-LP.

Characterization of BA-LP

The particle size of BA-LP produced by the optimal process prescription was 236.97 ± 3.89 nm, the PDI was 0.287 ± 0.022, and the EE was 86.03% ± 0.41 (Figure 2A). TEM examination of BA-LP morphology revealed a spherical nanoparticle, and the size of the particles assessed using the TEM images was in agreement with the measured particle size (Figure 2B). The stability test over 14 days showed that there was no significant change in the particle size and PDI of BA-LP, indicating good stability of BA-LP. We also tested the EE of BA in liposomes over 14 days, and the rate of change in EE was not significant, indicating that water-insoluble BA was encapsulated in liposomes with no leakage over 14 days (Figure 2C and D).

Preparation of BA-LG

The results of the study on the effect of different concentrations of CS solution and β-GP solution on the gelling temperature and gelling time of the gels are shown in Tables 1 and 2. The results show that with the increase of CS solution and β-GP concentration, the gelling temperature of the gel decreases and the gelling time is shortened. However, considering that the gel needs to be adapted to the body temperature, and the characteristics of too high concentration of β-GP solution is easy to precipitate, so the subsequent preparation process should be selected as the optimal concentration of CS solution concentration of 2% and β-GP solution concentration of 60%.

The results of the examination of the effects of different CS solution and β-GP solution mixing volume ratios on the gelling temperature and gelling time of the hydrogels are shown in Table 3, which shows that the gelling temperature of the gels decreases and the gelling time shortens with the increase of the volume ratio of the β-GP solution in the mixing of the two solutions. When the volume ratio of CS solution to β-GP solution is 4:1, the gelling temperature and time at this time are ideal, so this level is selected as the optimal condition.

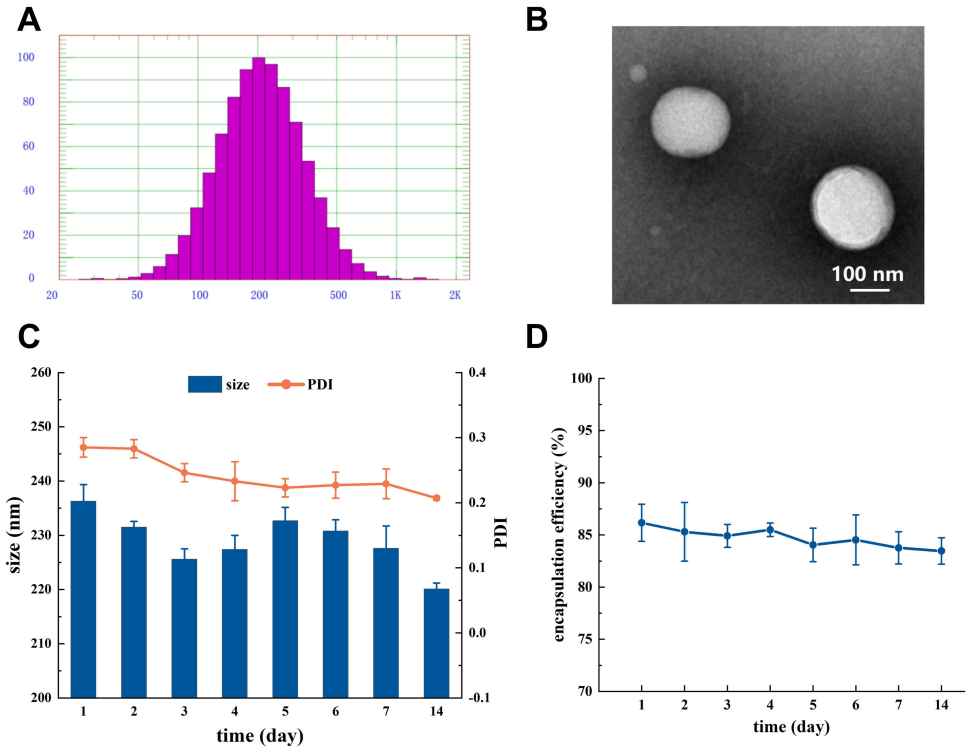

Figure 2 Characterization of BA-LP. (**A**) Particle size distribution of BA-LP. (**B**) TEM images of BA-LP. Scale bar = 100 nm. (**C**) BA-LP particle size and PDI for 7 days (n=3). (**D**) Encapsulation efficiency stability of BA-LP in 7 days (n=3).

In vitro Release Properties of Liposome-Hydrogel Systems and BA

The loading of different drugs is shown in Figure 3A. a. Blank-Gel at room temperature; b. Blank-Gel after gelation at 37 °C in a water bath; c. BA-LP at room temperature; d. BA-LG at room temperature; e. BA-LG after gelation at 37 °C in a water bath. It can be seen that at room temperature, Blank-Gel, BA-LP and BA-LG are all sols or liquids with fluidity, while at 37°C, Blank-Gel and BA-LG are solidified solid colloids. This suggests that BA-LG has temperature-sensitive properties due to the cross-linking of CS with β-GP.[62]

Table 1 Effect of Chitosan Concentration ($\overline{X} \pm s$, n=3)

Chitosan Concentration (%)	Gelation Temperature (°C)	Gelation Time (s)
0.75	42.0±0.33	556.3±40.4
1	40.5±0.31	413.3±40.4
1.5	39.0±0.27	316.6±30.5
2	36.5±0.30	153.7±32.1
2.5	35.5±0.29	113.3±30.6

Table 2 Effect of β-GP Concentration ($\overline{X} \pm s$, n=3)

β-GP Concentration (%)	Gelation Temperature (°C)	Gelation Time (s)
40	38.5±0.26	403.3±20.8
60	37.0±0.29	133.3±15.3
80	36.0±0.18	420.0±20.0

https://doi.org/10.2147/IJN.S516572

Table 3 Effect of CS to β-GP Volume Ratio ($\overline{X} \pm s$, n=3)

CS to β-GP Volume Ratio	Gelation Temperature (°C)	Gelation Time (s)
3:1	35.5±0.28	196.7±20.8
4:1	36.5±0.33	202.4±18.5
5:1	37.5±0.31	206.7±15.3
9:1	40.5±0.24	453.3±15.3

Relative to BA-Free and BA-LP, the in vitro release results showed that BA-LG had a more pronounced slow-release effect, with BA-Free reaching nearly complete release at 4 h, whereas BA-LG had a cumulative release of 60% at 24 h (Figure 3B). The results showed that BA-LG exhibited a more pronounced slow-release effect.

From the cumulative release curves (Figure 3C) of transdermal release, the cumulative penetration increased nearly twofold in the BA-LP and BA-LG groups compared with the BA-Free group. This was different from the results of in vitro release, probably because of the better penetration of liposomes into the skin barrier. It is noteworthy that the cumulative release after 12 h was higher in the BA-LG group than in the BA-LP group, probably because the action of the gel ensured a long residence time and sustained slow release of the drug on the skin surface. The results showed that the transdermal delivery of BA can be improved by loading it into liposomal gels.

The above results suggest that BA-LG can continuously release drugs, maintain the concentration of drugs on the skin surface, and thus prolong the duration of drug action. This is very important for patients with UV damage who need long-term symptom relief, as it can reduce the frequency of medication administration and improve patient compliance.

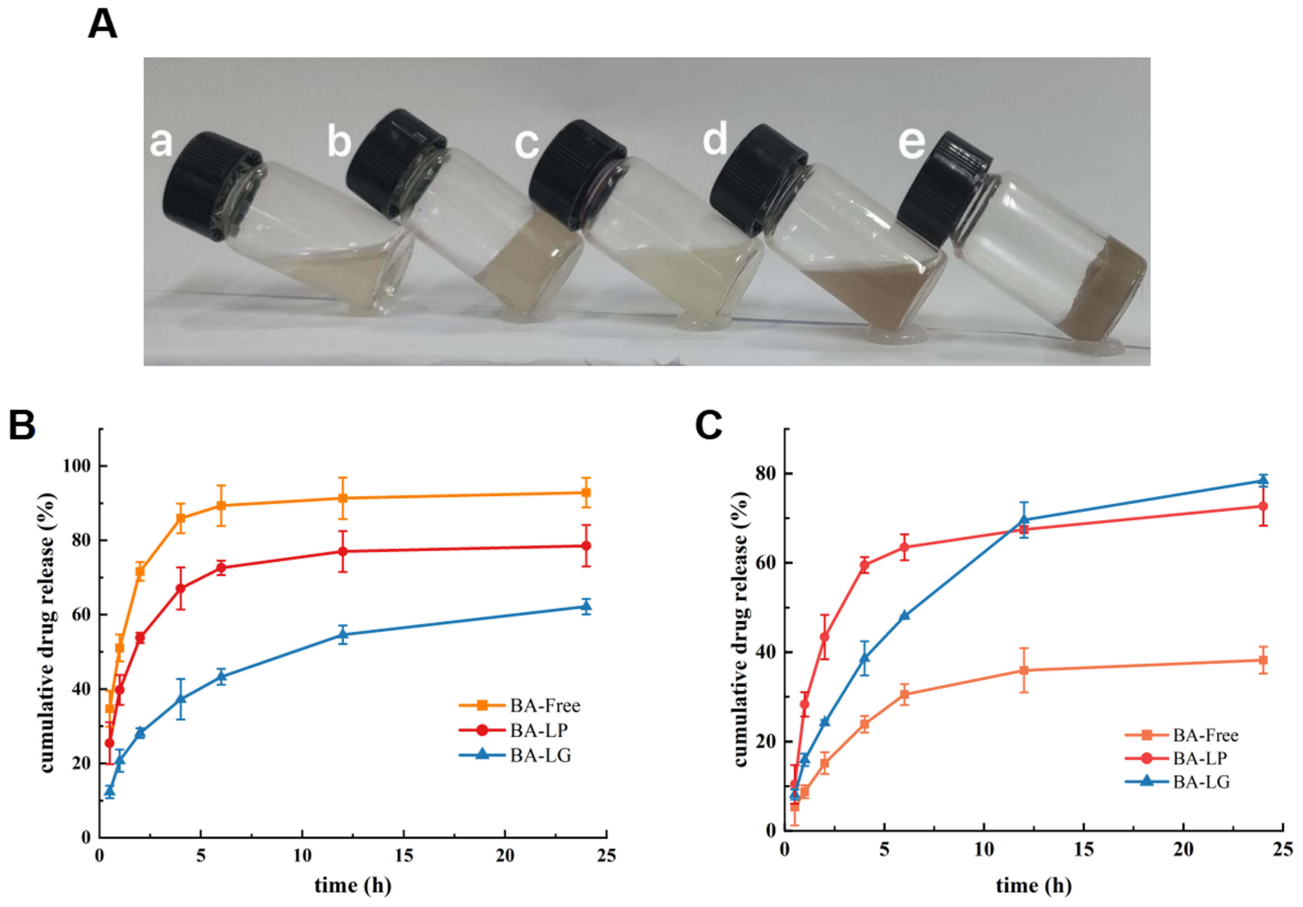

Figure 3 (**A**) The state of hydrogels at different temperatures (a. Blank-Gel at room temperature; b. Blank-Gel after gelation at 37 °C in a water bath; c. BA-LP at room temperature; d. BA-LG at room temperature; e. BA-LG after gelation at 37 °C in a water bath). (**B**) The in vitro release of BA from BA-Free, BA-LP and BA-LG in PBS of pH 7.2 (n=3). (**C**) The transdermal release of Baicalin of BA from BA-Free, BA-LP and BA-LG (n=3).

Temperature-Sensitive Properties of Liposome-Hydrogel Systems

The pH of BA-LG was determined to be near neutral in the range of 7.08 ± 0.03. As shown in Figure 4A, at room temperature, BA-LG was in the state of gray-yellow opaque sol, and the hydrogel was visually homogeneous, smooth and delicate. Take an appropriate amount of BA-LG in the palm of your hand and rub it slightly, the hydrogel is smooth and wet with viscosity, strong variability, and no particles present. The state of BA-LG before and after rubbing is shown in Figure 4B. This shows that its homogeneity is good. At 37 °C, the gelling time of the Blank-Gel was 126.7±20.8 s, and that of BA-LG was 113.3±15.3 s, with a moderate gelling rate. Then using a syringe to inject the hydrogel, BA-LG can be easily injected and words written, and the gel sticks firmly and stays connected to the vessel's bottom when inverted (Figure 4C). Therefore, this indicates good injectability and adhesion of the formed BA-LG.

Two portions of BA-LG were stained with methylene blue and basic fuchsin respectively, and placed in a test tube and gelled in a water bath at 37°C to obtain a solid cylindrical gel. Then they were divided into half cylinders respectively and combined. After 48 h of resting, the colors of the two parts of the gel blended, indicating that BA-LG still has good diffusion ability in the solid state (Figure 4D). The ductility results of BA-LG are shown in Figure 4E.

Characterization of Liposome-Hydrogel Systems

SEM can clearly display its micro scale-oriented pore structure and nano scale fiber network structure. SEM examination showed that the gel surface was loose and porous, and that the loading of BA liposomes caused the honeycomb-like structure on the gel surface to disappear (Figure 5). The loading of BA-LP may lead to chemical cross-linking, hydrogen bond formation, and space-filling effects in the hydrogel, thereby altering the network structure of the hydrogel and causing the disappearance of the honeycomb-like structure.

In vitro Cytotoxicity Studies

To assess the safety for the application of the prepared gels, an in vitro cytotoxicity test was carried. The results of the CCK-8 assay showed that BA-LP and BA-LG were not toxic to human skin glial cell line HaCaT when the concentration was below 100 μg/mL (Figure 6A).

Using a Transwell experiment, the gel was co-cultured with HaCaT to further validate that the Blank-Gel and BA-LG had no effect on the morphology of the cells and exhibited no cytotoxicity (Figure 6B and C), and that the BA-LG gel could be safely applied.

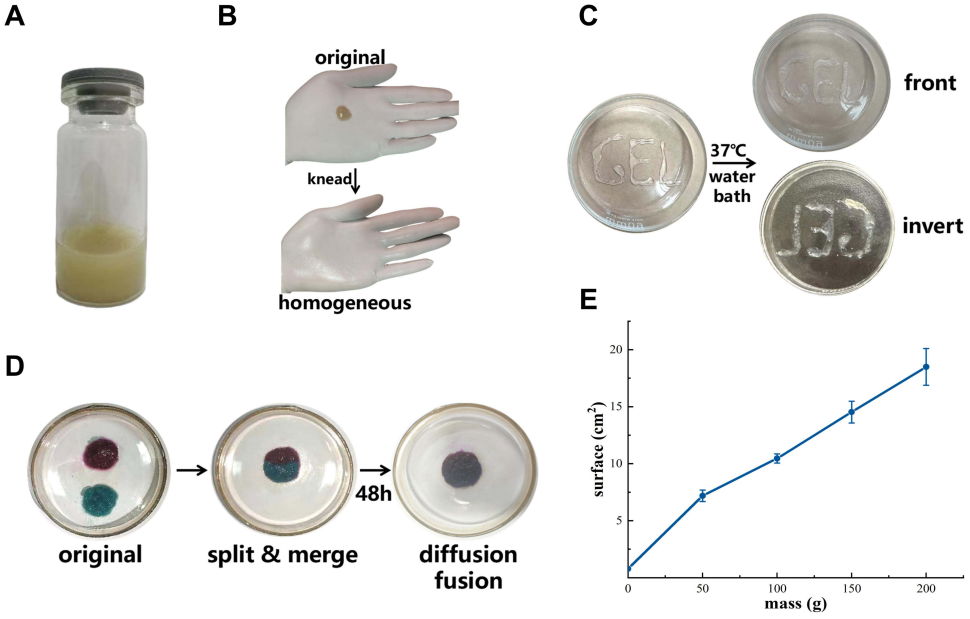

Figure 4 The appearance (**A**), homogeneity (**B**), injectability (**C**), adhesion (**C**), diffusivity (**D**), and spreadability (**E**, n=3) of BA-LG.

https://doi.org/10.2147/IJN.S516572

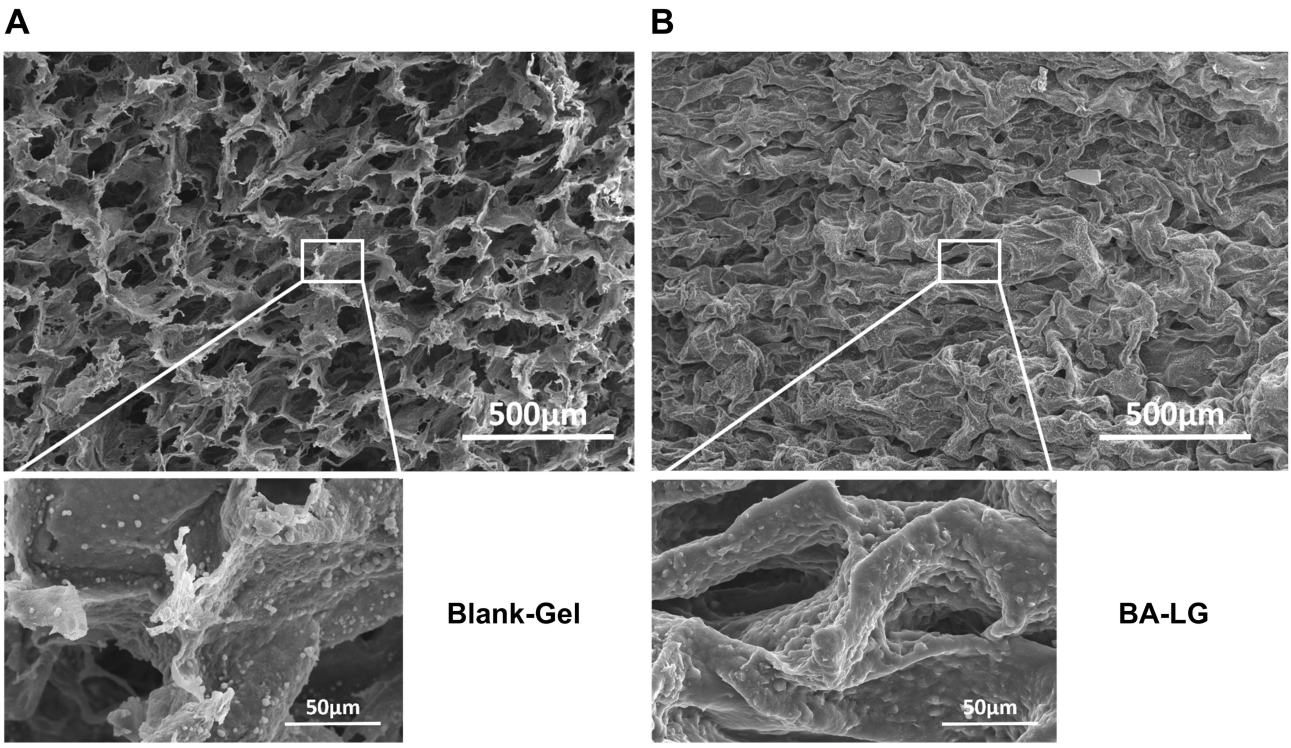

Figure 5 SEM images of Blank-Gel (**A**) and BA-LG (**B**). Scale bar = 50 and 500 μm.

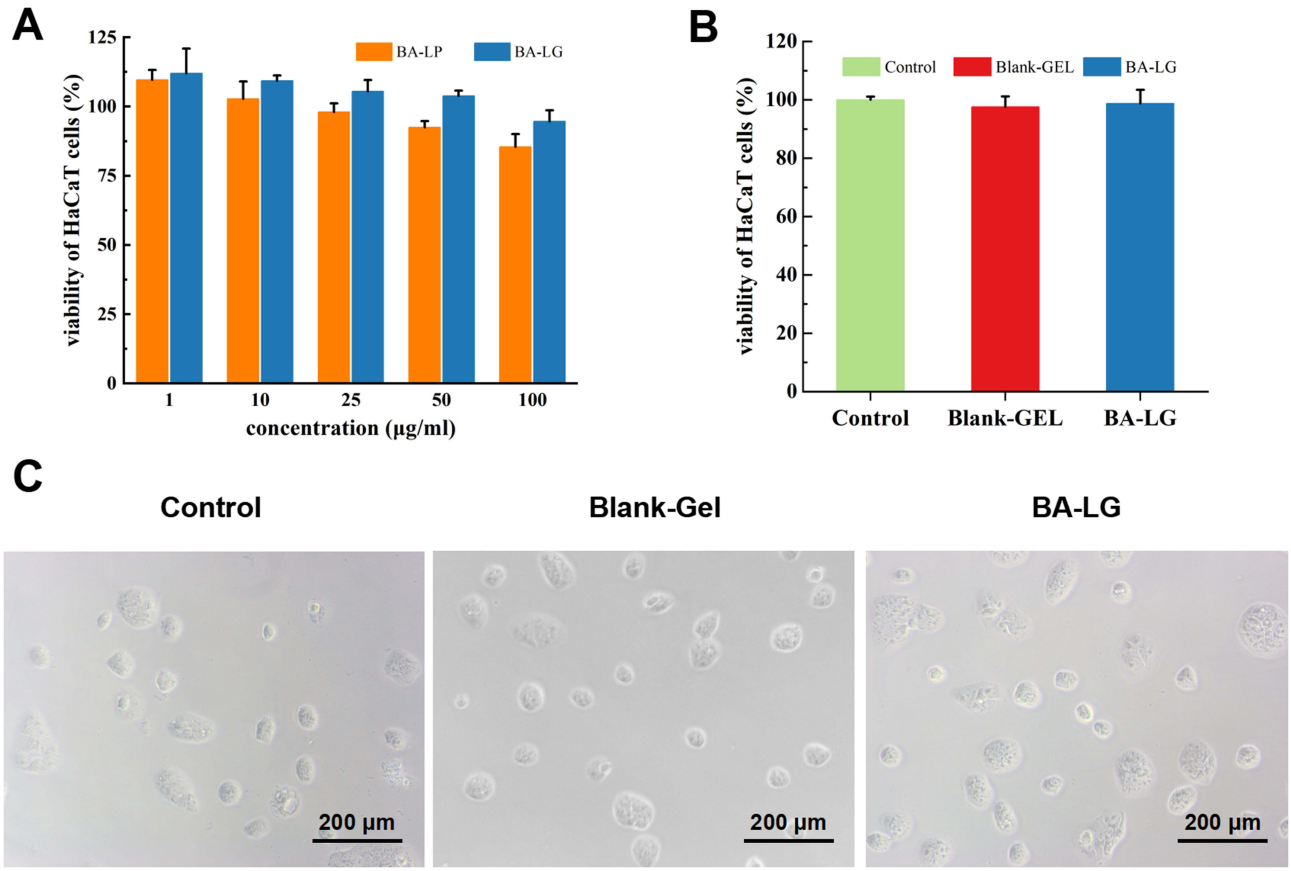

Figure 6 In vitro safety of BA-LG. (**A**) CCK-8 of BA-LP and BA-LG on HaCaT cells. (**B**) Transwell model of Blank-Gel and BA-LG on HaCaT cells. (**C**) Images of HaCaT cells after Blank-Gel and BA-LG treatment. Scale bar = 200 μm.

BA-LG Liposome-Hydrogel System Reduces UV Damage to Skin

In the UVB-induced skin damage model in mice, the Control group had smooth skin with no damage, whereas the Model group showed damage such as erythema and skin wrinkles. The BA-Free-treated group showed better skin condition than the Model group; however, this group still had significant damage, whereas the BA-LG-treated group showed comparatively lesser damage (Figure 7).

BA-LG Liposome-Hydrogel System Reduces UV Oxidative Damage to Skin

H&E and Masson staining showed better skin morphology and structure in the BA-LP and BA-LG groups than in the Model group, further demonstrating the protective effect of BA on the skin (Figure 8A). In the tissue sections stained with H&E and Masson, compared to the control group, the H&E staining of the model group (Model) shows thickened epidermis, increased cell layers, and possible infiltration of inflammatory cells, indicating pathological damage. Meanwhile, Masson staining reveals irregular distribution of collagen fibers and an increase in blue areas, indicating increased collagen deposition, which may reflect the process of fibrosis or repair after injury. The H&E staining of the BA-free group (BA-Free) shows that the epidermal thickness may have recovered compared to the model group, but there may still be slight cell layer disorder or signs of inflammation. Masson staining shows that the distribution of collagen fibers may have improved, but there may still be some irregularities or excessive deposition. The H&E staining of the BA-LG group (BA-LG) shows that the epidermal thickness is close to that of the control group, with orderly cell arrangement and significantly reduced signs of inflammation, indicating that BA-LG treatment may effectively improve tissue damage. Masson staining shows that the distribution of collagen fibers is close to normal, with even blue area distribution, indicating that the collagen fiber structure has been well restored and the degree of fibrosis has been reduced. This suggests that the BA-LG temperature-sensitive gel system protects the cells from damage and reduces the number of inflammatory cells and collagen loss.

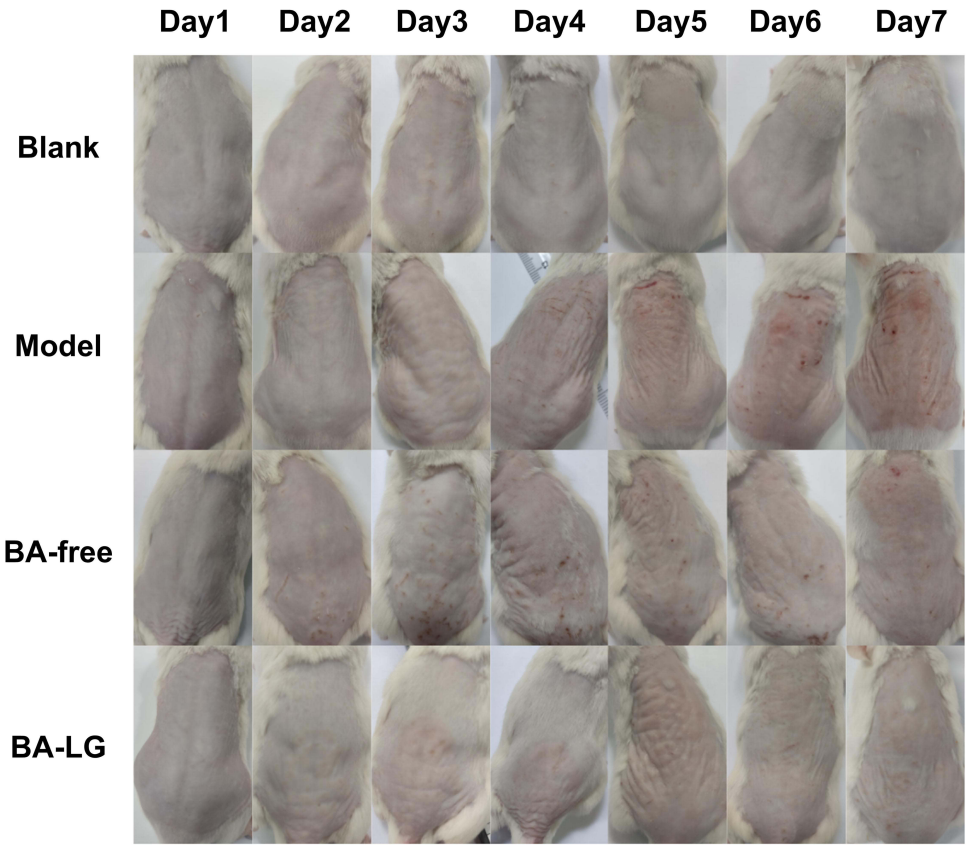

Figure 7 Images of skin UV damage in mice 7 days after treatment with BA-LP and BA-LG.

https://doi.org/10.2147/IJN.S516572

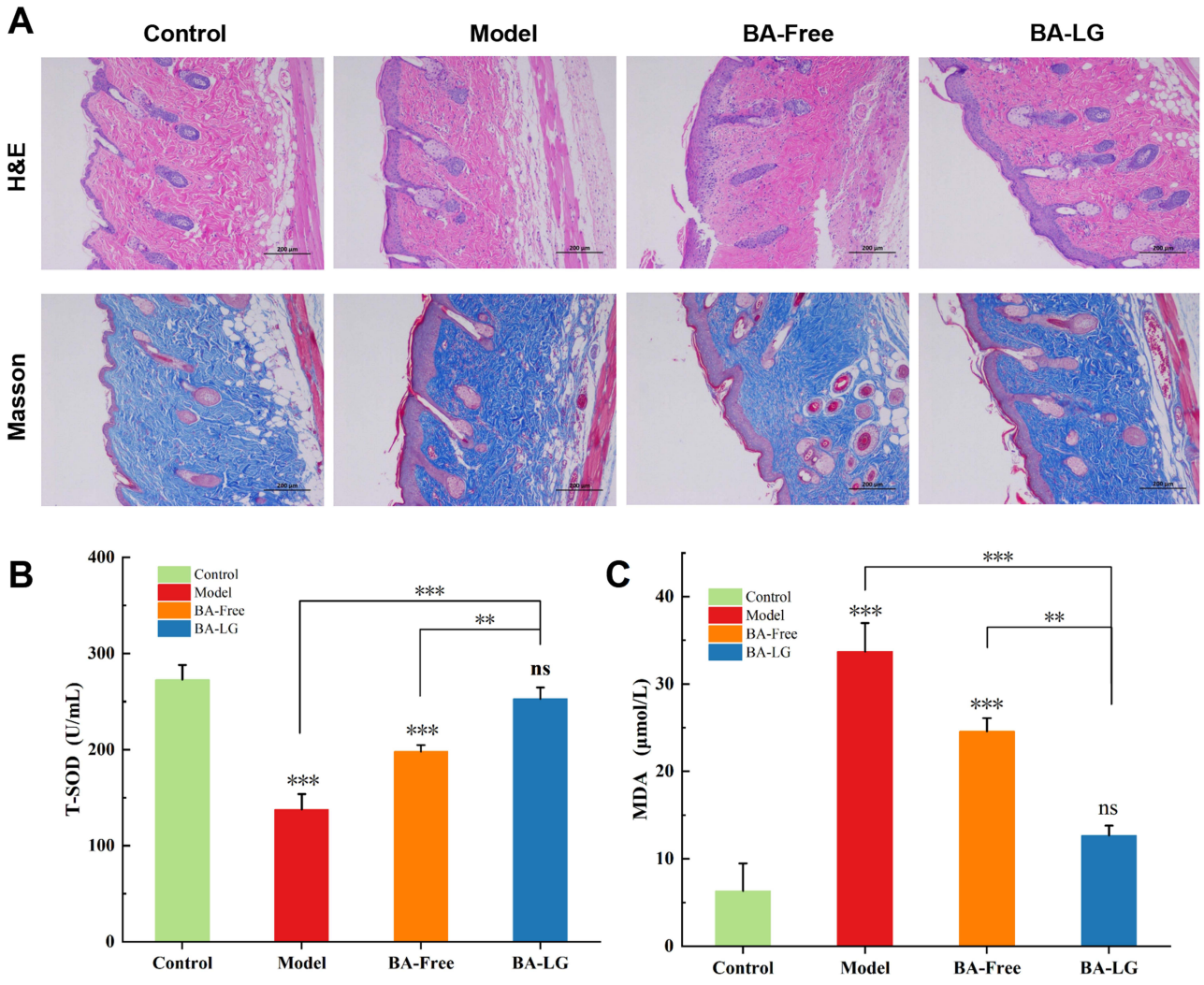

Figure 8 Therapeutic effect of BA-LG on ultraviolet damage of mouse skin. (**A**) Micrographs of H&E and Masson staining of mice skin tissues after BA-Free and BA-LG treatment. Scale bar =200 μm. (**B**) T-SOD content in different groups after UV damage (**p < 0.01, ***p < 0.001). (**C**) MDA content in different groups after UV damage (**p < 0.01, ***p < 0.001).

Further physicochemical tests showed that the use of BA-LG restored SOD activity in mouse skin and reduced skin MDA damage, which in turn led to the reduction of oxidative damage, thus protecting the skin from UVB photodamage (Figure 8B and C).

Anti-Inflammatory Effects of BA-LG

UVB irradiation of the skin upregulates inflammatory cytokines and related factors, leading to skin damage. As shown in Figure 9, after UVB irradiation, the inflammatory factors IL-6, PGE2 and TNF-α were significantly increased in the skin tissues of mice in the model group, which indicated that UVB irradiation induced the expression of inflammatory factors in the skin of mice. After treatment with BA-LG, the inflammatory factors in the skin of mice were significantly reduced to normal levels, indicating that BA-LG has a certain anti-inflammatory effect and can protect the skin from UV damage by inhibiting the expression of inflammatory factors.

Conclusion

In this study, liposomes loaded with BA (BA-LP) were prepared by a thin-film dispersion technique using cholesterol and soy lecithin as raw materials, and the optimal prescription process for BA-LP was devised using a one-factor investigation. Then

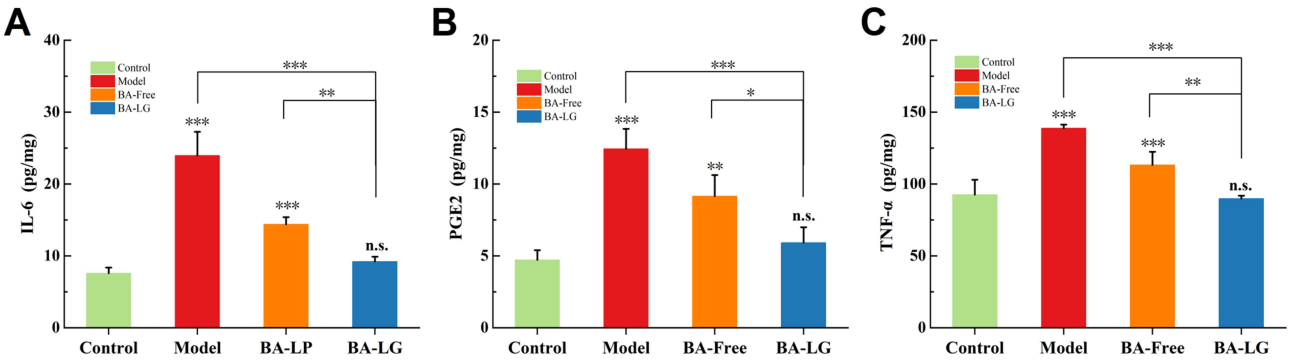

Figure 9 Levels of IL-6 (**A**), PGE2 (**B**) and TNF-α (**C**) in skin tissues of mice in different treatment groups (*p < 0.1, **p < 0.01, ***p < 0.001).

a novel injectable temperature-sensitive liposome hydrogel loaded with BA was developed using β-GP as a cross-linking agent to induce CS to form a temperature-sensitive hydrogel. The formulation exhibited good stability, injectability, temperature sensitivity, slow-release effects, and biosafety. In the UVB photodamage model, BA-LG protects the skin from UVB photodamage by restoring skin SOD activity, reducing MDA content, and inhibiting the expression of IL-6, PGE2 and TNF-α inflammatory factors, thereby reducing oxidative damage to the skin. This study demonstrated the promising application of BA as a treatment for UV-induced skin photodamage and validated the feasibility of using BA-LG as a new delivery system for drug administration to the skin.

Abbreviations

UV, ultraviolet; BA, baicalin; BA-LP, baicalin liposomes; MDA, malondialdehyde; SOD, superoxide dismutase; β-GP, β-glycerophosphate; HPLC, high-performance liquid chromatography; TEM, transmission electron microscopy; BA-LG, baicalin temperature-sensitive liposome hydrogel.

Acknowledgments

This work was supported by Foundation of National Natural Science Foundation of China (82404939) and National Natural Science Foundation of Sichuan (24NSFSC1834). We would like to thank Editage (www.editage.cn) for English language editing.

Disclosure

The authors report no conflicts of interest in this work.

References

1. Eyerich S, Eyerich K, Traidl-Hoffmann C, et al. Cutaneous barriers and skin immunity: differentiating a connected network. *Trends Immunol*. 2018;39(4):315–327. doi:10.1016/j.it.2018.02.004
2. Lim K-M. Skin epidermis and barrier function. *Int J Mol Sci*. 2021;22(6):3035.
3. Wang X, Mao Y. Emerging ultraviolet persistent luminescent materials. *Adv Opt Mater*. 2022;10(21). doi:10.1002/adom.202201466
4. Chen C-Y, Chen C-J, Lai C-H, et al. Increased matriptase zymogen activation by UV irradiation protects keratinocyte from cell death. *J Dermatol Sci*. 2016;83(1):34–44. doi:10.1016/j.jdermsci.2016.03.006
5. Schuch AP, Moreno NC, Schuch NJ, et al. Sunlight damage to cellular DNA: focus on oxidatively generated lesions. *Free Radic Biol Med*. 2017;107:110–124.
6. Lan -C-CE, Hung Y-T, Fang A-H, et al. Effects of irradiance on UVA-induced skin aging. *J Dermatol Sci*. 2019;94(1):220–228. doi:10.1016/j.jdermsci.2019.03.005
7. Battie C, Jitsukawa S, Bernerd F, et al. New insights in photoaging, UVA induced damage and skin types. *Exp Dermatol*. 2014;23(s1):7–12. doi:10.1111/exd.12388
8. Yin Y, Li W, Son Y-O, et al. Quercitrin protects skin from UVB-induced oxidative damage. *Toxicol Appl Pharmacol*. 2013;269(2):89–99. doi:10.1016/j.taap.2013.03.015
9. Svobodová AR, Galandáková A, Šianská J, et al. DNA damage after acute exposure of mice skin to physiological doses of UVB and UVA light. *Arch Dermatol Res*. 2012;304(5):407–412. doi:10.1007/s00403-012-1212-x
10. Neale RE, Lucas RM, Byrne SN, et al. The effects of exposure to solar radiation on human health. *Photochem Photobiol Sci*. 2023;22(5):1011–1047. doi:10.1007/s43630-023-00375-8

11. Miligi L. Ultraviolet radiation exposure: some observations and considerations, focusing on some Italian experiences, on cancer risk, and primary prevention. *Environments*. 2020;7(2):10. doi:10.3390/environments7020010
12. Farjadmand F, Karimpour-Razkenari E, Nabavi SM, et al. Plant polyphenols: natural and potent UV-protective agents for the prevention and treatment of skin disorders. *Mini-Rev Med Chem*. 2021;21(5):576–585. doi:10.2174/1389557520666201109121246
13. Wen Y, Wang Y, Zhao C, et al. The pharmacological efficacy of baicalin in inflammatory diseases. *Int J Mol Sci*. 2023;24(11):9317. doi:10.3390/ijms24119317
14. Wang D, Li Y. Pharmacological effects of baicalin in lung diseases. *Front Pharmacol*. 2023;14:1188202.
15. Wang L, Xian Y-F, Loo SKF, et al. Baicalin ameliorates 2,4-dinitrochlorobenzene-induced atopic dermatitis-like skin lesions in mice through modulating skin barrier function, gut microbiota and JAK/STAT pathway. *Bioorg Chem*. 2022;119:105538. doi:10.1016/j.bioorg.2021.105538
16. Ishfaq M, Wu Z, Wang J, et al. Baicalin alleviates Mycoplasma gallisepticum-induced oxidative stress and inflammation via modulating NLRP3 inflammasome-autophagy pathway. *Int Immunopharmacol*. 2021;101:108250. doi:10.1016/j.intimp.2021.108250
17. Li D, Lin B, Yusuf N, et al. Proteomic analysis and functional studies of baicalin on proteins associated with skin cancer. *Am J Chin Med*. 2017;45(03):599–614. doi:10.1142/S0192415X17500355
18. Liu Z, Dang B, Li Z, et al. Baicalin attenuates acute skin damage induced by ultraviolet B via inhibiting pyroptosis. *J Photochem Photobiol B Biol*. 2024;256:112937. doi:10.1016/j.jphotobiol.2024.112937
19. Chen Y, Song S, Wang Y, et al. Potential mechanism of oral baicalin treating psoriasis via suppressing Wnt signaling pathway and inhibiting Th17/IL −17 axis by activating PPARγ. *Phytother Res*. 2022;36(10):3969–3987. doi:10.1002/ptr.7546
20. Wang W, Xin X, Zhang M, et al. Improving physicochemical characteristics and cytotoxicity of baicalin esters by liposome encapsulation. *J Microencapsul*. 2024;41(4):312–325. doi:10.1080/02652048.2024.2348462
21. Chen Y, Yang Y, Wang F, et al. Antiviral effect of baicalin phospholipid complex against duck hepatitis A virus type 1. *Poult Sci*. 2018;97(8):2722–2732. doi:10.3382/ps/pey155
22. Li Z, Liu Y, Wang J, et al. Baicalin-berberine complex nanocrystals orally promote the co-absorption of two components. *Drug Delivery Transl Res*. 2022;12(12):3017–3028. doi:10.1007/s13346-022-01167-w
23. Li X-Y, Shi L-X, Shi N-N, et al. Multiple stimulus-response berberine plus baicalin micelles with particle size-charge-release triple variable properties for breast cancer therapy. *Drug Dev Ind Pharm*. 2023;49(2):189–206. doi:10.1080/03639045.2023.2195501
24. Brito S, Baek M, Bin B-H. Skin structure, physiology, and pathology in topical and transdermal drug delivery. *Pharmaceutics*. 2024;16(11):1403. doi:10.3390/pharmaceutics16111403
25. Sivadasan D, Madkhali OA. The design features, quality by design approach, characterization, therapeutic applications, and clinical considerations of transdermal drug delivery systems—a comprehensive review. *Pharmaceuticals*. 2024;17(10):1346. doi:10.3390/ph17101346
26. Lee J, Hwang GW, Lee BS, et al. Artificial octopus-limb-like adhesive patches for cupping-driven transdermal delivery with nanoscale control of stratum corneum. *ACS Nano*. 2024;18(7):5311–5321.
27. Schafer N, Balwierz R, Biernat P, et al. Natural ingredients of transdermal drug delivery systems as permeation enhancers of active substances through the stratum corneum. *Mol Pharm*. 2023;20(7):3278–3297. doi:10.1021/acs.molpharmaceut.3c00126
28. Lunter D, Klang V, Eichner A, et al. Progress in topical and transdermal drug delivery research—focus on nanoformulations. *Pharmaceutics*. 2024;16(6):817. doi:10.3390/pharmaceutics16060817
29. Sobhani H, Karimi M, Alibolandi M, et al. Preparation and characterization of metformin-loaded transdermal formulations based on liquid crystalline lipid particles in diabetic-induced rats. *J Drug Delivery Sci Technol*. 2025;105:106634. doi:10.1016/j.jddst.2025.106634
30. Gunawan M, Bestari AN, Ramadon D, et al. Combination of lipid-based nanoparticles with microneedles as a promising strategy for enhanced transdermal delivery systems: a comprehensive review. *J Drug Delivery Sci Technol*. 2025;107:106807. doi:10.1016/j.jddst.2025.106807
31. Kushwaha P, Saxena S, Shukla B. A recent overview on dermatological applications of liposomes. *Recent Pat Nanotechnol*. 2021;15(4):310–321. doi:10.2174/1872210514666201021145233
32. Castañeda-Reyes ED, Perea-Flores MDJ, Davila-Ortiz G, et al. Development, characterization and use of liposomes as amphipathic transporters of bioactive compounds for melanoma treatment and reduction of skin inflammation: a review. *Int J Nanomed*. 2020;15:7627–7650. doi:10.2147/IJN.S263516
33. Wang T, Fang H, Yalikun S, et al. Pluronic F127-lipoic acid adhesive nanohydrogel combining with Ce3+/Tannic Acid/Ulinastatin nanoparticles for promoting wound healing. *Biomacromolecules*. 2023;25(2):924–940. doi:10.1021/acs.biomac.3c01060
34. Cao L, Qian X, Min J, et al. Cutting-edge developments in the application of hydrogels for treating skin photoaging. *Front Mater*. 2024;11. doi:10.3389/fmats.2024.1443514
35. Balintova L, Blazickova M, Sramkova M. Nanocomposite hydrogels in skin cancer medicine. *Neoplasma*. 2024;71(02):153–163. doi:10.4149/neo_2024_240315N118
36. Wang Z, Yuan J, Xu Y, et al. Olea europaea leaf exosome-like nanovesicles encapsulated in a hyaluronic acid / tannic acid hydrogel dressing with dual "defense-repair" effects for treating skin photoaging. *Mater Today Bio*. 2024;26:101103. doi:10.1016/j.mtbio.2024.101103
37. Gu R, Zhou H, Zhang Z, et al. Research progress related to thermosensitive hydrogel dressings in wound healing: a review. *Nanoscale Adv*. 2023;5(22):6017–6037. doi:10.1039/D3NA00407D
38. Peng C-L, Shih Y-H, Liang K-S, et al. Development of in situ forming thermosensitive hydrogel for radiotherapy combined with chemotherapy in a mouse model of hepatocellular carcinoma. *Mol Pharm*. 2013;10(5):1854–1864. doi:10.1021/mp3006424
39. Chen H, Xu J, Sun J, et al. Recent advances on thermosensitive hydrogels-mediated precision therapy. *Asian J Pharm Sci*. 2024;19(3).
40. Jing Z, Li W, Liao W, et al. Fructus xanthii and magnolia liliiflora volatile oils liposomes-loaded thermosensitive in situ gel for allergic rhinitis management. *Int J Nanomed*. 2024;19:1557–1570. doi:10.2147/IJN.S445240
41. Liu Y, Ma W, Zhou P, et al. In situ administration of temperature-sensitive hydrogel composite loading paclitaxel microspheres and cisplatin for the treatment of melanoma. *Biomed Pharmacother*. 2023;160:114380. doi:10.1016/j.biopha.2023.114380
42. Mardikasari SA, Budai-Szűcs M, Orosz L, et al. Development of thermoresponsive-gel-matrix-embedded amoxicillin trihydrate-loaded bovine serum albumin nanoparticles for local intranasal therapy. *Gels*. 2022;8(11):750. doi:10.3390/gels8110750
43. Rancan F, Asadian-Birjand M, Dogan S, et al. Effects of thermoresponsivity and softness on skin penetration and cellular uptake of polyglycerol-based nanogels. *J Control Release*. 2016;228:159–169.

44. Kurian AG, Singh RK, Sagar V, et al. Nanozyme-engineered hydrogels for anti-inflammation and skin regeneration. *Nano-Micro Lett*. 2024;16 (1):110.
45. Yin Y, Hu B, Yuan X, et al. Nanogel: a versatile nano-delivery system for biomedical applications. *Pharmaceutics*. 2020;12(3):290. doi:10.3390/pharmaceutics12030290
46. Adnan M, Afzal O, S. A. Altamimi A, et al. Development and optimization of transethosomal gel of apigenin for topical delivery: in-vitro, ex-vivo and cell line assessment. *Int J Pharm*. 2023;631:122506.
47. Adin SN, Gupta I, Aqil M, et al. Baicalin loaded transethosomes for rheumatoid arthritis: development, characterization, pharmacokinetic and pharmacodynamic evaluation. *J Drug Delivery Sci Technol*. 2023;81:104209.
48. Lu H, Ren S, Li X, et al. Poly(ethylene glycol)/chitosan/sodium glycerophosphate gel replaced the joint capsule with slow-release lubricant after joint surgery. *J Biomater Sci Polym Ed*. 2018;29(11):1331–1343. doi:10.1080/09205063.2018.1459351
49. Deng A, Kang X, Zhang J, et al. Enhanced gelation of chitosan/β-sodium glycerophosphate thermosensitive hydrogel with sodium bicarbonate and biocompatibility evaluated. *Mater Sci Eng C*. 2017;781:147–154.
50. de Lima JA, Paines TC, Motta MH, et al. Novel pemulen/Pullulan blended hydrogel containing clotrimazole-loaded cationic nanocapsules: evaluation of mucoadhesion and vaginal permeation. *Mater Sci Eng C*. 2017;79:886–893.
51. Duarah S, Durai RD, Narayanan VB. Nanoparticle-in-gel system for delivery of vitamin C for topical application. *Drug Delivery Transl Res*. 2017;7(5):750–760. doi:10.1007/s13346-017-0398-z
52. Meng C, Wei W, Wang Y, et al. Study of the interaction between self-assembling peptide and mangiferin and in vitro release of mangiferin from in situ hydrogel. *Int J Nanomed*. 2019;147:447–460.
53. Menon P, Teo YY, Misran M. Development and evaluation of dipalmitoyl phosphatidylcholine (DPPC) liposomal gel: rheology and in vitro drug release properties. *Korea Aust Rheol J*. 2023;36(1):45–54. doi:10.1007/s13367-023-00082-x
54. Liu H, Guo X, Yi T, et al. Frog skin derived peptides with potential protective effects on ultraviolet B–induced cutaneous photodamage. *Front Immunol*. 2021;12:613365.
55. He Y, Luo L, Liang S, et al. Influence of probe-sonication process on drug entrapment efficiency of liposomes loaded with a hydrophobic drug. *Int J Polym Mater Polym Biomater*. 2018;68(4):193–197. doi:10.1080/00914037.2018.1434651
56. Borges-Araújo L, Borges-Araújo AC, Ozturk TN, et al. Martini 3 coarse-grained force field for cholesterol. *J Chem Theory Comput*. 2023;19 (20):7387–7404. doi:10.1021/acs.jctc.3c00547
57. Nakhaei P, Margiana R, Bokov DO, et al. Liposomes: structure, biomedical applications, and stability parameters with emphasis on cholesterol. *Front Bioeng Biotechnol*. 2021;9. doi:10.3389/fbioe.2021.705886
58. Saeting K, Mitrevej A, Leuenberger H, et al. Development of alendronate niosomal delivery system for gastrointestinal permeability improvement. *J Drug Delivery Sci Technol*. 2022;67:102885. doi:10.1016/j.jddst.2021.102885
59. Hudiyanti D, Christa SM, Mardhiyyah NH, et al. Dynamics insights into aggregation of phospholipid species with cholesterol and vitamin C. *Pharmacia*. 2022;69(2):385–391. doi:10.3897/pharmacia.69.e81435
60. Kassab G, Manav N, Pires L, et al. Structural effect of rhenium- and iridium-complex liposome composition on their selectivity for antimicrobial photodynamic therapy. *Small Sci*. 2023;4(2). doi:10.1002/smsc.202300131
61. López RR, G. Font de Rubinat P, Sánchez L-M, et al. The effect of different organic solvents in liposome properties produced in a periodic disturbance mixer: transcutol®, a potential organic solvent replacement. *Colloids Surf B*. 2021;198:111447. doi:10.1016/j.colsurfb.2020.111447
62. Rahmati M, Samadikuchaksaraei A, Mozafari M. Insight into the interactive effects of β-glycerophosphate molecules on thermosensitive chitosan-based hydrogels. *Bioinspired Biomimetic Nanobiomater*. 2016;5(2):67–73. doi:10.1680/jbibn.15.00022